Waves at the nematic-isotropic interface: The role of surface tension anisotropy, curvature elasticity, and backflow effects

V. Popa-Nita* and P. Oswald†

Laboratoire de Physique de l'Ecole Normale Supérieure de Lyon, 46 Allée d'Italie, 69364 Lyon Cedex 07, France

(Received 2 July 2003; revised manuscript received 24 October 2003; published 31 December 2003)

Recently, a theoretical description of waves at the nematic-isotropic interface has been proposed using a generalized dynamical Landau–Ginzburg–de Gennes theory [V. Popa-Nita and T. J. Sluckin, Phys. Rev. E **66**, 041703 (2002)]. This calculation assumed an isotropic surface tension, i.e., independent of the director orientation at the interface and neglected all coupling between the director and the hydrodynamic flow. As a consequence, the director was assumed to keep a fixed orientation and do not couple with the oscillations of the interface. These assumptions are rather crude in real nematics where surface tension anisotropy may be as large as 20% and where hydrodynamic coupling with the director is known to be important. In this paper we propose to take into account these two effects: as a result, interface oscillations couple with the director field via hydrodynamic flows and backflow effects. We analyze how these phenomena change the dispersion relation. Finally, we review experiments on the nematic-isotropic interface and discuss how to measure experimentally the dispersion relation.

DOI: 10.1103/PhysRevE.68.061707 PACS number(s): 61.30.Cz, 64.70.Md, 83.80.Xz

I. INTRODUCTION

In this paper, we analyze the problem of the damping of capillary waves at the interface between two fluids. This classical problem is simple when the two fluids are isotropic and immiscible and when the interface thickness is much smaller than the wavelength of the undulation (''sharp-interface'' limit). On the other hand, the problem is more complicated when the two phases may transform into each other (interface between two phases of the same compound at the coexistence temperature), an effect that becomes dominant when the wavelength of the oscillation approaches the interface thickness. This phenomenon should be visible at the liquid-vapor interface close to the critical point, but experiments are very difficult in these conditions. It also exists in liquid crystals, where phase transitions are very often very weakly first order. This was pointed out recently by one of us (V.P.-N.) and Sluckin in Ref. [1], where the nematic-isotropic interface was analyzed. In this particular example, it was shown that the dispersion relation of the capillary waves deviates strongly from its usual form (found in the hydrodynamic sharp-interface limit) at short wavelength (typically smaller than $1-2$ μm, which should be visible experimentally). Nevertheless, this calculation was not complete as it neglected the coupling between the nematic director and the hydrodynamic flow, as well as the anchoring effect of the director at the interface.

The goal of this paper is to analyze the influence of these two effects on the dispersion relation of capillary waves at the nematic-isotropic (N-I) interface. As in Ref. [1], we will use a phase-field formulation [2]. In this approach, the free-boundary problem associated with the sharp-interface model is replaced by a coupled pair of nonlinear reaction-diffusion equations. The spatial and temporal variations of the order parameter phase field is governed by a time-dependent Ginzburg-Landau (TDGL) equation. The second equation (for temperature) is based on a modification of the heat equation, and contains a source term that mimics latent heat production at the moving interface.

Interfaces in thermotropic liquid crystals behave like model systems in which the phase-field theory can be used particularly well. In their cases, the phase-field order parameter is not an *ad hoc* invention, as it can be physically measured. In addition, the fluidity of liquid crystals renders accessible a large range of time scales in experiments. The relevant phase-field theory of the nematic-isotropic phase transition [3,4] we will use in this paper is a dynamical generalization of the familiar Landau–de Gennes theory [5,6], in which coupling with hydrodynamics has been included. The corresponding equations have been first proposed by Hess [7] and subsequently completed by Olmsted and Goldbart [8] and by Qian and Sheng [9].

Apart from its intrinsic interest, the dynamics of liquid crystal interfaces is much richer than in usual systems (such as solid-liquid interfaces or surfaces in contact with air or vacuum). The reason is that the corresponding phase transitions can usually be described by a nonconserved order parameter (associated with the symmetry breaking at the transition) and are weakly first order. The nematic-isotropic transition, where the orientational order parameter is quadrupolar, belongs to this category. In this example, it has been shown that very different dispersion relations for waves at the nematic-isotropic interface can be obtained depending on the way the calculations are done: more precisely, the diffuse interface theory, solved by assuming that the order parameter and velocity fields do not interact, leads to purely diffusive surface waves whose mode structure is identical to that of the bulk diffusive modes found in the TDGL theory [4]. On the other hand, the sharp-interface theory yields modified capil-

*Permanent address: Faculty of Physics, University of Bucharest, P.O. Box MG-11, Bucharest 76900, Romania.

†Author to whom correspondence should be addressed. Email address: patrick.oswald@ens-lyon.fr

lary waves, with a large propagating component.

In a previous paper [1], these two points of view have been reconciled by analyzing the surface eigenmodes of the nematic-isotropic interface within the Hess-Olmsted-Goldbart model. To simplify things, it was assumed in that paper that the nematic director was fixed in space and time, so that the relevant physics was only described by a scalar order parameter. It turns out that this assumption is only valid if the surface tension is isotropic (i.e., does not depend on the director orientation at the interface), and, less obvious, if the coupling between the flow and the director (and possible ''backflow'' effects) can be neglected. A general dispersion relation was then obtained, having as particular cases the (scalar) order parameter relaxation regime in the short wavelength limit and the viscous damping regime valid in the long wavelength limit.

In this paper, we reconsider this problem in a more general way, by taking into account both the hydrodynamic coupling with the director and the surface tension anisotropy, which we know to be very large at the nematic-isotropic interface. In this case, the problem is more complicated as the director oscillates. To introduce the anchoring energy of the director at the interface, we have included the L_2 Ginzburg term in the elastic free energy in addition to the isotropic one L_1 [see Eq. (4) below]. This term fixes the strength of the anchoring energy at the nematic-isotropic interface. We emphasize that, in this model, the preferred orientation of the director with respect to the interface is either parallel or normal depending on the sign of L_2. In the following we shall assume L_2 is positive, which favors homeotropic anchoring.

To calculate the general dispersion relation of nematic-isotropic interface, we start from a generalization of the standard Ericksen-Leslie (EL) [10,11] theory written in term of tensorial order parameter [9]. This new formulation involves the same number of viscous parameters as in the EL theory, which can be expressed as linear combinations of the Leslie viscosities.

In order to perform the calculations, we assume that the base state of the system is a planar nematic-isotropic interface in equilibrium. This condition fixes its temperature at $T_{N\text{-}I}$, the nematic-isotropic phase transition temperature. To simplify, we further assume that the temperature is uniform (no temperature gradient perpendicular to the interface). Due to thermal fluctuations, small-amplitude monochromatic waves develop at the interface. A linear stability analysis of the equations is used to obtain their dispersion relation.

The paper is organized as follows. In Sec. II we describe the basic model and give the governing equations. We then present in Sec. III the dispersion relations corresponding to the two regions defined by the typical lengths in the problem. The general dispersion relation and numerical results are presented in Sec. IV. The differences with the simplified model treated in Ref. [1] are emphasized in Sec. V, which is followed by a general discussion of the results in Sec. VI. Experiments on the nematic-isotropic front are reviewed then in Sec. VII, where we also make a few suggestions for measuring the dispersion relation. Finally, in Sec. VIII, we draw some conclusions and present directions for future work.

II. EQUATIONS OF MOTION

The local state of a uniaxial nematic liquid crystal is described by a traceless symmetric second-rank tensor $Q_{\alpha\beta}$,

$$Q_{\alpha\beta}=S(3n_\alpha n_\beta-\delta_{\alpha\beta})/2, \tag{1}$$

where the unit vector $\vec{n}$ is the nematic director and S the usual scalar order parameter ($S=0$ in the isotropic liquid and $S=1$ in a fully oriented nematic phase).

Within the mesoscopic approach, the Landau–de Gennes (LdG) free energy functional is given by [12,13]

$$F(Q,\nabla Q,T)=\int [f(Q,T)+f_F(\nabla Q)]dV, \tag{2}$$

where

$$f(Q,T)=a(T-T^*)Q_{\alpha\beta}Q_{\beta\alpha}-BQ_{\alpha\beta}Q_{\beta\gamma}Q_{\gamma\alpha}+C(Q_{\alpha\beta}Q_{\beta\alpha})^2 \tag{3}$$

is the bulk LdG free energy density and

$$f_F(\nabla Q)=\tfrac{1}{2}L_1(\partial_\alpha Q_{\beta\gamma})^2+\tfrac{1}{2}L_2(\partial_\alpha Q_{\alpha\beta})^2 \tag{4}$$

the distortion (elastic) free energy density.

We assume that the heat diffusion is sufficiently rapid in order that the system remains at thermal equilibrium. We therefore ignore the equation for energy conservation and assume that the system does not shift from temperature $T_{N\text{-}I}$. We further assume the fluid is incompressible. Within these approximations, the equations of motion for the velocity and the order parameter become [9]

$$\partial_\alpha v_\alpha=0, \tag{5}$$

$$\rho\frac{dv_\alpha}{dt}=\partial_\beta(-p\,\delta_{\alpha\beta}+\sigma^d_{\alpha\beta}+\sigma^v_{\alpha\beta}), \tag{6}$$

$$0=h_{\alpha\beta}+h^v_{\alpha\beta}-\lambda\,\delta_{\alpha\beta}-\epsilon_{\alpha\beta\gamma}\lambda_\gamma, \tag{7}$$

where ρ is the density, p the pressure, while λ and λ_γ are the Lagrange multipliers associated with conditions $\mathrm{Tr}\,Q=0$ and $Q_{\alpha\beta}=Q_{\beta\alpha}$, respectively. In this expression, α, β, and γ run from 1 to 3, summation over repeated indices is implied, $\epsilon_{\alpha\beta\gamma}$ is the Levi-Civita symbol, and d/dt is the total time derivative $\partial/\partial t+\vec{v}\cdot\nabla$. The distortion stress σ^d and the elastic molecular field h are obtained in standard manner as

$$\sigma^d_{\alpha\beta}=-\frac{\partial F}{\partial(\partial_\alpha Q_{\gamma\rho})}\partial_\beta Q_{\gamma\rho}, \tag{8}$$

$$h_{\alpha\beta}=-\delta F/\delta Q_{\alpha\beta}. \tag{9}$$

As for the viscous stress tensor σ^v and the viscous molecular field h^v, they are given by a tensorial generalization of the EL theory [9],

$$\sigma^v_{\alpha\beta}=\beta_1 Q_{\alpha\beta}Q_{\mu\nu}A_{\mu\nu}+\beta_4 A_{\alpha\beta}+\beta_5 Q_{\alpha\mu}A_{\mu\beta}+\beta_6 Q_{\beta\mu}A_{\mu\alpha}+\tfrac{1}{2}\mu_2 N_{\alpha\beta}-\mu_1 Q_{\alpha\mu}N_{\mu\beta}+\mu_1 Q_{\beta\mu}N_{\mu\alpha}, \tag{10}$$

$$-h^{v}_{\alpha\beta}=-\tfrac{1}{2}\mu_2 A_{\alpha\beta}+\mu_1 N_{\alpha\beta}, \tag{11}$$

where

$$N_{\alpha\beta}=\frac{dQ_{\alpha\beta}}{dt}+Q_{\alpha\mu}W_{\mu\beta}-W_{\alpha\mu}Q_{\mu\beta} \tag{12}$$

is the time rate of change of the order parameter with respect to the background fluid angular velocity (corotational derivative in the language of rheologists). β_1, β_4, β_5, β_6, μ_1, and $\mu_2=\beta_6-\beta_5$ are viscous coefficients which can be expressed in terms of the Leslie coefficients α_i and the value of the order parameter S [9], while $A_{\alpha\beta}=\frac{1}{2}(\partial_\alpha v_\beta+\partial_\beta v_\alpha)$ and $W_{\alpha\beta}=\frac{1}{2}(\partial_\alpha v_\beta-\partial_\beta v_\alpha)$ are, respectively, the symmetric and antisymmetric parts of the velocity gradient tensor.

Let us now define the two typical lengths of the problem and the associated characteristic times.

(i) The first length is related to the order parameter itself. It strongly varies across the interface over a typical distance known as the microscopic correlation length $l_S=(16CL/B^2)^{1/2}\simeq 10^{-6}$ cm, where $L=3(L_1+L_2/6)/2$ is a linear combination of the two stiffness constants L_1 and L_2. This length gives the typical width of the order parameter profile within the interface. The order parameter S is also associated with a typical relaxation time $t_S=24C\mu_1/B^2\simeq 10^{-6}$ s . This time does not depend on the size of the region in which the order parameter has been disturbed, as S is not a hydrodynamic variable.

(ii) The second length is associated with the vorticity, i.e., to the flow induced by the motion of the interface. The corresponding physics is described by the generalized Navier-Stokes equation (6), which can be considered in the thin interface limit. The important physical parameters are the capillary force, associated with the interfacial tension γ, the viscous dissipation, associated with some viscosity coefficient η, and the fluid inertia, governed by the mass density ρ. From these three quantities, we can construct only one length $l_\eta=\eta^2/\rho\gamma\simeq 1$ cm .

In order to find the physical meaning of this length, let us consider a perturbation of size l at the interface and let us estimate its relaxation time. This perturbation creates a pressure gradient inside the fluid given by the Laplace equation: $\nabla P\simeq\gamma/l^2$. This pressure gradient is balanced in the Navier-Stokes equation, either by the inertial term or by the viscous term, depending on the value of l. Let τ be the relaxation time: in the former case, we have $\gamma/l^2\simeq\rho l/\tau^2$, which gives the inertial typical relaxation time $\tau_i\simeq(\rho l^3/\gamma)^{1/2}$; in the latter case, $\gamma/l^2\simeq\eta(l/\tau)/l^2=\eta/\tau l$, which gives the typical viscous relaxation time $\tau_v\simeq\eta l/\gamma$. One immediately checks that the length l_η defined above gives the size of the perturbation for which the two relaxation times are equal $\tau_i=\tau_v=t_\eta=\eta^3/\rho\gamma^2$. So, for $l\gg l_\eta$, $\tau_i\gg\tau_v$, which means that inertia dominates. In contrast, for $l\ll l_\eta$, $\tau_v\gg\tau_i$, meaning that now viscosity dominates. In conclusion, l_η is the length scale separating the inertial regime from the viscous one. In the following, we shall use t_η as unit time, which is the typical relaxation time of a perturbation of size l_η. Note that in our system $l_\eta\simeq 1$ cm and $t_\eta\simeq 10$ s are pretty large (in comparison with what we would obtain for an ordinary liquid-air interface) as the *N-I* interface surface tension is very small.

In the following, the ratio of these two lengths $\epsilon=l_S/l_\eta\simeq 10^{-6}$ will constitute the small parameter of the theory.

We consider a two-dimensional flow with horizontal and vertical velocity components u and w in the x and z directions, respectively, ϕ is the angle between the director and the z axis $[\vec{n}=(\sin\phi(x,z,t),0,\cos\phi(x,z,t))\simeq(\phi(x,z,t),0,1)]$ and we simplify the expressions (10) and (11) by assuming that

$$\beta_1=\beta_5=\beta_6=0,\quad \beta_4=2\beta, \tag{13}$$

which give $\mu_2=0$ [9]. In terms of Leslie coefficients α_i, these relations are equivalent to

$$\alpha_1=\alpha_5=\alpha_6=0,\quad -\alpha_2=\alpha_3=\alpha=9S^2\mu_1/4,$$
$$\alpha_4=\beta_4=2\beta. \tag{14}$$

Note that similar approximations were used to describe backflows effects in the Smectic-*C* films and were known for preserving all the physics of the problem (even if the hypothesis $-\alpha_2=\alpha_3$, corresponding to a ''tumbling'' nematic, is rarely observed, except very close to a smectic phase) [13]. Within these approximations, the coefficient β describes the dissipation due to shear flow (shear viscosity), while μ_1 is associated with the dissipation due to the rotational motion of the optical axis (with the standard rotational viscosity $\gamma_1=\alpha_3-\alpha_2=9S^2\mu_1/2$). Using these hypotheses and Eqs. (1)–(4), the basic Eqs. (5)–(7) take the form

$$0=\partial_x u+\partial_z w, \tag{15}$$

$$\rho\frac{du}{dt}=-\partial_x p+\frac{1}{2}\left(\frac{9S^2_{\rm nem}}{4}\mu_1+2\beta\right)\nabla^2 u-\frac{9S^2_{\rm nem}\mu_1}{4}\partial^2_{zt}\phi-L\nabla^2 S\partial_x S, \tag{16}$$

$$\rho\frac{dw}{dt}=-\partial_z p+\frac{1}{2}\left(\frac{9S^2_{\rm nem}}{4}\mu_1+2\beta\right)\nabla^2 w+\frac{9S^2_{\rm nem}\mu_1}{4}\partial^2_{xt}\phi-L\nabla^2 S\partial_z S, \tag{17}$$

$$\frac{9S^2_{\rm nem}\mu_1}{2}\frac{d\phi}{dt}=\frac{9(2L_1+L_2)S^2_{\rm nem}}{4}\nabla^2\phi+\frac{9S^2_{\rm nem}\mu_1}{4}(\partial_z u-\partial_x w), \tag{18}$$

$$\frac{\mu_1}{2}\frac{dS}{dt}=h^{[s]}_{zz}+h^{[s]}_{xx}, \tag{19}$$

where $h^{[s]}_{xx}=\frac{1}{3}df/dS-\frac{1}{3}L\nabla^2 S-\frac{1}{4}L_2\nabla^2 S$ and $h^{[s]}_{zz}=-\frac{2}{3}df/dS+\frac{2}{3}L\nabla^2 S+\frac{1}{2}L_2\partial^2_{zz}S$ [with $df/dS=3a(T-T^*)S-\frac{9}{4}BS^2+9CS^3$] are the symmetric traceless components of the elastic molecular field given by Eq. (9),

$L=3(L_1+L_2/6)/2$ and $S_{\rm nem}=B/6C$ is the value of S in the nematic phase at temperature $T_{N\text{-}I}$. Note that in writing Eqs. (15)–(19), we have neglected the terms of the following types: $S(\partial_\alpha S)(\partial_\beta\phi)$ and $\phi(\partial_\alpha S)(\partial_\beta S)$ which appear in the distortion stress tensor. The terms of the first type cancel due to the fact that in the region of the dimension l_S, ϕ is constant and in the region of the dimension l_η, S is constant (ϕ relaxes to its equilibrium value over a distance of the dimension l_η). The terms of the second type are negligible (because ϕ is always very close to zero, assuming homeotropic anchoring) comparing with terms of the form $(\partial_\alpha S)(\partial_\beta S)$ which have been considered in the distortion stress tensor. Equation (17) and the first three terms on the right hand side of Eqs. (15) and (16) are written treating the orientational order parameter $S_{\rm nem}$ as a frozen constant. We define $\alpha=9S_{nem}^2\mu_1/4$, $K=9(2L_1+L_2)S_{nem}^2/4$, and $\eta=(\alpha+2\beta)/2$ and we rewrite Eqs. (15)–(19) in dimensionless forms by measuring length in unit of l_η, time in unit of t_η, and introducing the dimensionless quantities: $\bar{S}=S/S_{\rm nem}=6CS/B$, $\tau=24a(T-T_{N\text{-}I})C/B^2=(T-T_{N\text{-}I})/(T_{N\text{-}I}-T^*)$, $\bar{f}=24^2C^3f/B^4$, $\bar{\rho}=24^2\rho C^3\gamma^2/B^4\eta^2$, $\bar{p}=24^2C^3p/B^4$, $\bar{\eta}=24^2C^3\eta/t_\eta B^4$, $\bar{K}=24^2C^3K/B^4l_\eta$, $\bar{\mu}_1=3\eta\mu_1/2\rho L$, $\bar{\alpha}=24^2C^3\alpha/t_\eta B^4$, and $\epsilon^2=l_S^2/l_\eta^2$. Omitting the bar notation in the following, the governing Eqs. (15)–(19) can be written as

$$0=\partial_x u+\partial_z w, \tag{20}$$

$$\rho\frac{du}{dt}=-\partial_x p+\eta\nabla^2 u-\alpha\partial_{zt}^2\phi-\epsilon^2\nabla^2 S\partial_x S, \tag{21}$$

$$\rho\frac{dw}{dt}=-\partial_z p+\eta\nabla^2 w+\alpha\partial_{xt}^2\phi-\epsilon^2\nabla^2 S\partial_z S, \tag{22}$$

$$2\alpha\frac{d\phi}{dt}=K\nabla^2\phi+\alpha(\partial_z u-\partial_x w), \tag{23}$$

$$\epsilon^2\mu_1\frac{dS}{dt}=-\frac{df}{dS}+\epsilon^2\left(1+\frac{3L_2}{4L}\right)\nabla^2 S-\frac{3}{2}\epsilon^2\frac{L_2}{L}\partial_{xx}^2 S, \tag{24}$$

where $df/dS=2(1+\tau)S-6S^2+4S^3$.

This form of the free energy density describes a first-order nematic-isotropic phase transition. For $\tau=\tau_{N\text{-}I}=0$, the two phases, nematic ($S_{\rm nem}=1$) and isotropic ($S_{\rm iso}=0$), coexist in equilibrium ($f_{\rm nem}=f_{\rm iso}$). In the following we suppose that the stationary planar nematic-isotropic interface (the base state of the system) is situated at $z=0$, such that the nematic lies in the region $z<0$ and the isotropic phase in the region $z>0$. As for x axis, it is taken in the direction of the wave vector $\vec{k}$ of the perturbation along the interface. This is possible without loss of generality, as the system is isotropic in x and y directions (neglecting the biaxiality of the nematic phase). In this way, the wave number k represents the modulus of the two-dimensional wave vector in the plane of the interface.

III. ASYMPTOTICS

We seek solutions of Eqs. (20)–(24) for $\epsilon\ll 1$, in the inner region (of dimension l_S) in which the order parameter varies rapidly (the solution is essentially diffusive) and in the outer region (of dimension l_η) in which the physics is governed by hydrodynamics (dissipation by shear flow and by rotation of the optical axis, respectively).

A. Outer region

In the outer region, S is constant in each phase ($S=S_{\rm nem}=1$ for $z<0$ and $S=S_{\rm iso}=0$ for $z>0$) and the equations for velocity and angle are the same for all orders in an expansion in ϵ. We have to consider separately the two phases.

1. Nematic phase

In the outer region of the nematic phase ($z<0$), $S=S_{\rm nem}=1$ and the working equations (20)–(24) become

$$0=\partial_x u+\partial_z w, \tag{25}$$

$$\rho\frac{du}{dt}=-\partial_x p+\eta\nabla^2 u-\alpha\partial_{zt}^2\phi \tag{26}$$

$$\rho\frac{dw}{dt}=-\partial_z p+\eta\nabla^2 w+\alpha\partial_{xt}^2\phi \tag{27}$$

$$2\alpha\frac{d\phi}{dt}=K\nabla^2\phi-\alpha(\partial_z u-\partial_x w). \tag{28}$$

Thus, the outer problem is equivalently with the EL continuum theory of the nematic liquid crystals and Eqs. (25)–(28) are similar to those used to study the transient periodic distortions which sometimes develop during the Fredericks transition [14,15]. The solution corresponding to the stationary planar interface is given by $u_0=w_0=0$, $p_0=$const, and $\phi_0=0$ assuming that homeotropic anchoring is favored. We now impose a small periodic sinusoidal perturbation to the interface of the form $\xi_I=\xi_k\exp(ikx-\Omega t)$, where ξ_I is the vertical displacement of the interface with respect to its equilibrium position $z=0$. In our notations, k is the wave vector (real number) and Ω is the angular frequency. The latter quantity is generally a complex number whose real part gives the relaxation time $\tau=1/{\rm Re}(\Omega)$ of the wave and the imaginary part the phase velocity $v_p={\rm Im}(\Omega)/k$. We then look for the solution of Eqs. (25)–(28) in the form $u=U_0\exp(qz+ikx-\Omega t)$, $w=W_0\exp(qz+ikx-\Omega t)$, $p=p_0+P_0\exp(qz+ikx-\Omega t)$, and $\Phi=\Phi_0\exp(qz+ikx-\Omega t)$. After substitution in Eqs. (25)–(28), we get a system of algebraic equations for the amplitudes

$$\begin{aligned}
&ikU_0+qW_0=0,\\
&[\rho\Omega-\eta(k^2-q^2)]U_0-ikP_0+q\alpha\Omega\Phi_0=0,\\
&[\rho\Omega-\eta(k^2-q^2)]W_0-qP_0+ik\alpha\Omega\Phi_0=0,\\
&\alpha qU_0-ik\alpha W_0+[2\alpha\Omega-K(k^2-q^2)]\Phi_0=0.
\end{aligned} \tag{29}$$

Putting the determinant of system (29) equal to zero, we obtain the following bulk characteristic equation, connecting q, k, and Ω:

$$(k^2-q^2)\{[2\alpha\Omega-K(k^2-q^2)][\rho\Omega-\eta(k^2-q^2)]+\alpha^2\Omega(k^2-q^2)\}=0, \tag{30}$$

with solutions

$$q=k \quad \text{and} \quad q^2=l_{1,2}^2=k^2-\frac{2\alpha\beta+K\rho\pm[4\alpha^2\beta^2+K^2\rho^2+4\alpha\rho K(\beta-2\alpha)]^{1/2}}{2K\eta}\Omega. \tag{31}$$

For a nematic of large depth (region $-\infty<z<0$), the wavelike solutions of Eqs. (25)–(28) are of the form

$$u=(ikAe^{kz}-l_1\hat{C}_1e^{l_1z}-l_2\hat{C}_2e^{l_2z})\exp(ikx-\Omega t), \tag{32}$$

$$w=(kAe^{kz}+ik\hat{C}_1e^{l_1z}+ik\hat{C}_2e^{l_2z})\exp(ikx-\Omega t), \tag{33}$$

$$p=p_0+\rho\Omega Ae^{kz}\exp(ikx-\Omega t), \tag{34}$$

$$\phi=(\phi_1\hat{C}_1e^{l_1z}+\phi_2\hat{C}_2e^{l_2z})\exp(ikx-\Omega t), \tag{35}$$

where $\phi_i=[\rho\Omega-\eta(k^2-l_i^2)]/\alpha\Omega=-\alpha(k^2-l_i^2)/[2\alpha\Omega-K(k^2-l_i^2)]$, $\hat{C}_i=C/(k^2-l_i^2)$, with $i=1,2$. In Eqs. (32)–(35) the velocity field may be decomposed in two parts: (i) a potential (irrotational) flow of amplitude proportional to A [which derivates from the potential $\psi=A\exp(kz+ikx-\Omega t)$] and (ii) a rotational flow of amplitude proportional to C that derivates from a vector potential.

2. Isotropic phase

In the isotropic phase (region $z>0$) the working equations (20)–(24) become

$$0=\partial_x u+\partial_z w, \tag{36}$$

$$\rho\frac{du}{dt}=-\partial_x p+\eta_I\nabla^2 u, \tag{37}$$

$$\rho\frac{dw}{dt}=-\partial_z p+\eta_I\nabla^2 w. \tag{38}$$

Thus, the outer problem of the isotropic phase is equivalent with the Navier-Stokes equations subject to the incompressibility condition [16–19].

Similar to the nematic phase, we get the wavelike solutions for the isotropic phase of large depth (region $0<z<\infty$) in the form

$$u'=(ikA'e^{-kz}+l\hat{C}e^{-lz})\exp(ikx-\Omega t), \tag{39}$$

$$w'=(-kA'e^{-kz}+ik\hat{C}e^{-lz})\exp(ikx-\Omega t), \tag{40}$$

$$p'=p_0+\rho\Omega A'e^{-kz}\exp(ikx-\Omega t), \tag{41}$$

where $l=k(1-\rho\Omega/\eta_I k^2)^{1/2}$.

3. Dispersion relation

Equations (32)–(35) and (39)–(41) correspond to the classical sharp-interface approach, where it is assumed that the thickness of the inner region is zero. In this limit, the dispersion relation is determined by the boundary conditions at the nematic-isotropic interface which can be taken at $z=0$ due to the smallness of the amplitude of the oscillations [16,17]. These conditions are as follows:

(i) and (ii) The x and z components of the velocity must be continuous.

(iii) The tangential components of the stress tensor must also be continuous, which gives $\sigma_{xz}=\sigma'_{xz}$, where $\sigma_{xz}=\beta(\partial_x w+\partial_z u)-\frac{1}{2}K\nabla^2\phi$ and $\sigma'_{xz}=\eta_I(\partial_x w'+\partial_z u')$ are the xz components of the stress tensor in the nematic phase and the isotropic liquid, respectively.

(iv) As to the jump of the normal component of the stress tensor, it is given by the Laplace law

$$\sigma_{zz}-\sigma'_{zz}=\gamma\frac{\partial^2\xi_I}{\partial x^2}, \tag{42}$$

where $\sigma_{zz}=-p+2\beta\partial_z w$ and $\sigma'_{zz}=-p'+2\eta_I\partial_z w'$ are the normal component of the stress at the interface in the nematic phase and in the isotropic liquid, respectively. In this equation, $\xi_I=-(1/\Omega)w|_{z=0}$ corresponds to the displacement of the interface at point x with respect to the plane $z=0$ (with $\langle\xi_I\rangle=0$).

(v) The last boundary condition is given by the surface torque equation

$$K_{eff}\partial_z\phi|_{z=0}+W_a(\phi+\delta)=0, \tag{43}$$

where W_a is the anchoring energy, $\delta=d\xi_I/dx$ is the small tilt angle of the interface about the x axis, and $K_{eff}=K+2K_4$. The first term in Eq. (43) is the elastic torque acting on the director at the surface [assuming $K_1=K_3=K$ and taking into account the surface like term $K_4\vec{\nabla}\cdot(\vec{n}\vec{\nabla}\cdot\vec{n}+\vec{n}\times\vec{\nabla}\times\vec{n})$] [13] and the second one is the anchoring torque due to the surface tension anisotropy. After substituting solutions (32)–(35) and (39)–(41) into the boundary conditions, we obtain a homogeneous system of equations for the five amplitudes A, A', $\hat{C}_1$, $\hat{C}_2$, and $\hat{C}$. Equating to zero its determinant gives the dispersion relation in the form

$$\Omega_{\beta\alpha}^2=\frac{D}{N}\Omega_0^2, \tag{44}$$

where $D=(k-l)(F_2E_1-F_1E_2)+(k^2-l^2)[2k(F_2-F_1)+F_1(l_2+l)-F_2(l_1+l)]$ and $N=l(F_1E_2-F_2E_1)+(k^2-l^2)[(F_1+k^2/\Omega)(l_2+l)-(F_2+k^2/\Omega)(l_1+l)]+k^2/2\Omega[(l_2+l)E_1-(l_1+l)E_2]$. Here $E_i=l^2-l_i^2-K(k^2-l_i^2)\phi_i/2\beta$, $F_i=(bl_i+1)\phi_i$, b is a parameter defined as $b=K_{eff}/W_a$, and $\Omega_0^2=-\gamma k^3/2\rho$ is the capillary wave dispersion relation for ideal (inviscid) fluids. To obtain Eq. (44), we have considered that the densities and translational viscosities of the two phases are equal ($\beta=\eta_I$). The subscript $\beta\alpha$ recalls that the real part of Ω is associated with the dissipation due to the shear flow and the rotational motion of the director (which induces supplementary backflow effects). Note that in the limit $W_a\to 0$ and $\alpha\to 0$, the director orientation does not change in time (it is fixed because there is no coupling with the flow and the interface), so that the dispersion relation greatly simplifies and becomes

$$\Omega_\beta^2=\frac{l-k}{l}\Omega_0^2, \tag{45}$$

as found in Ref. [1]. Note that we only use the subscript β in this equation to show that the real part of Ω is simply due in this case to the shear flow.

Before calculating the full dispersion relation, we now need to analyze the problem in the ''inner'' region, i.e., at a length scale of the order of the interface thickness l_S.

B. Inner region

At small scale, hydrodynamics are negligible. By using inner variables $\zeta=x/\epsilon$ and $\xi=z/\epsilon$, the leading order equations for the order parameter are obtained from the general equations (29), (25), and (26) and write as follows:

$$\tilde{\mu}_1\frac{\partial S}{\partial t}=-\frac{df}{dS}+\left(1+\frac{3L_2}{4L}\right)\nabla^2 S-\frac{3L_2}{2L}\partial_{\zeta\xi}^2 S, \tag{46}$$

$$0=-\partial_\zeta p-\nabla^2 S\partial_\zeta S, \tag{47}$$

$$0=-\partial_\xi p-\nabla^2 S\partial_\xi S, \tag{48}$$

where $\tilde{\mu}_1=24C\mu_1/B^2$. The first equation gives the order parameter profile and will be used to calculate the dispersion relation in the inner region. The two others allow calculating the pressure field, which we will not give explicitly. In the following we set $\tilde{\zeta}=\zeta/(1+3L_2/4L)^{1/2}$ and $\tilde{\xi}=\xi/(1+3L_2/4L)^{1/2}$. In these new variables, Eq. (46) simplifies and becomes (omitting the tilde signs in the following)

$$\mu_1\frac{\partial S}{\partial t}=-\frac{df}{dS}+\nabla^2 S-\frac{6L_2}{4L+3L_2}\partial_{\zeta\xi}^2 S, \tag{49}$$

where, now, units of length and time are $l_S'=l_S(1+3L_2/4L)^{1/2}$ and t_η, respectively. For the equilibrium planar nematic-isotropic interface perpendicular to ξ axis, the solution of TDGL equation (49) with boundary conditions $S_0(-\infty)=1$ and $S_0(\infty)=0$ (the subscript 0 refers to the equilibrium interface) is given by

$$S_0(\xi)=\frac{1}{2}\left(1-\tanh\frac{\xi}{\sqrt{2}}\right), \tag{50}$$

where we have fixed the center of the interface (defined by $S_0=1/2$) at $\xi=0$. Correspondingly, the surface tension (for homeotropic anchoring) is given (in the dimensionless form) by

$$\gamma=\int_{-\infty}^{\infty}\left(\frac{dS_0}{d\xi}\right)^2 d\xi=\frac{\sqrt{2}}{6}. \tag{51}$$

Returning to real variables this equation takes the form

$$\gamma=\frac{\sqrt{2}}{6}\frac{B^3}{24^{3/2}C^{5/2}}L^{1/2}. \tag{52}$$

Similar calculation can be done by assuming that the director makes an angle ϕ with the z axis at the interface. In this case the surface tension becomes

$$\gamma(\phi)=\frac{\sqrt{2}}{6}\frac{B^3}{24^{3/2}C^{5/2}}\left(L+\frac{1}{2}L_2\sin^2\phi\right)^{1/2}. \tag{53}$$

At small surface tension anisotropy (L_2 much smaller than L), this equation can be rewritten in the Rapini-Popoular form

$$\gamma(\phi)=\gamma+\frac{1}{2}W_a\sin^2\phi, \tag{54}$$

with $L_2/L=2W_a/\gamma$. As a consequence, knowing γ and W_a allows us to calculate L and L_2. We note that in the case $L_2=0$, $W_a=0$, and $K_4=-K/2$ [see Eq. (58) below and Ref. [13], p. 246) and the boundary condition (43) is identically satisfied.

We now return to the dispersion relation in the inner region. It is obtained perturbing the base state, Eq. (50), by $S(\zeta,\xi,t)=S_0(\xi)+\mathcal{S}(\xi)\exp(ik\zeta-\Omega t)$. Substituting this form into Eq. (49) and linearizing in perturbation, give

$$H\mathcal{S}=\Omega\mathcal{S}, \tag{55}$$

where $H=-d_z^2+k^2[1-6L_2/(4L+3L_2)]+d^2f/dS^2(S_0)$ can be conveniently thought of as a quantum mechanical Hamiltonian operator [22]. Note that $d^2f/dS^2(S_0)$ is positive at $\xi=\pm\infty$ (where $S_0=0$ and $S_0=1$) and negative at $\xi=0$ (where $S_0=1/2$). In our case $f(S)=S^2(1-S)^2$, one has $d^2f/dS^2(S_0)=2-12S_0(\xi)+12S_0^2(\xi)$, which equals -1 at $\xi=0$, and tends to $+2$ for $\xi\to\pm\infty$. It follows that $d^2f/dS^2(S_0)$ represents a potential well which must have at least one bound state. In fact, since $k=0$ corresponds to a uniform translation of the interface, we know that $\Omega_{k=0}=0$ is the eigenvalue with the eigenfunction $d_\xi S_0$ [this can be easily checked by differentiating Eq. (61) with respect to ξ]. Also, since this function has no node, it must be the ground state. Since the k dependence of H is simply the additive constant $k^2[1-6L_2/(4L+3L_2)]$, it follows that $dS_0/d\xi$ is,

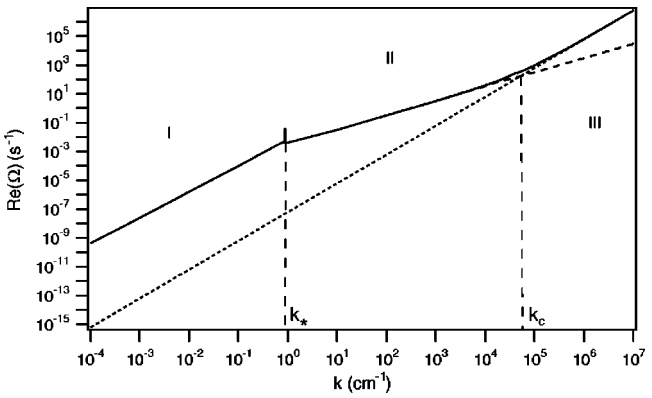

FIG. 1. The damping rate $\mathrm{Re}(\Omega)$ as a function of the wave vector k in a log-log plot defining three distinct regimes. The general dispersion relation, Eq. (57) (continuous curve), the viscous damping dispersion relation, Eq. (44) (dashed curve), and the order parameter relaxation dispersion relation, Eq. (56) (dotted curve). Region I—dissipation due to shear flow; region II—dissipation due to rotational motion of the director; Region III—relaxation of the order parameter.

for all k, the ground state eigenfunction—the so-called ''slow mode''—of eigenvalue (in ''real units'')

$$\Omega_S=\frac{4L}{9\mu_1}\left(1-\frac{6L_2}{4L+3L_2}\right)k^2. \tag{56}$$

We note that Ω_S is real and positive. It gives the relaxation rate of the order parameter in the absence of hydrodynamical coupling.

IV. GENERAL DISPERSION RELATION

In order to obtain the full dispersion relation, we need to match the solutions obtained in the outer and in the inner regions, respectively, at first order in ϵ^2. Similar matching was already done in Ref. [1] and we refer to that paper for detailed calculations. Using the same procedure, we obtain the generalized dispersion relation

$$\Omega^2-\Omega_S\Omega=\Omega_{\beta\alpha}^2, \tag{57}$$

where $\Omega_{\beta\alpha}$ and Ω_S are given by the Eqs. (44) and (56), respectively.

The real part of the solution of Eq. (57) and its asymptotic limits given by Eqs. (44) and (56) are drawn in Fig. 1. To perform the numerical calculations we have taken $L_1=3.63\times10^{-7}$ dyn, $L_2=3.69\times10^{-8}$ dyn, $L=5.53\times10^{-7}$ dyn, $K_4=-1\times10^{-7}$ dyn, $K_{eff}=1.02\times10^{-8}$ dyn, $b=2.03\times10^{-5}$ cm, which gives $\Omega_S=6.13\times10^{-7}k^2$. These parameters have been obtained by using the following equations:

$$\frac{L_2}{L}=2\frac{W_a}{\gamma},\quad K=\frac{9}{4}(2L_1+L_2)S_{\mathrm{nem}}^2,\quad K_4=-\frac{9}{4}L_1S_{\mathrm{nem}}^2,$$

$$L=\frac{3}{2}\left(L_1+\frac{L_2}{6}\right), \tag{58}$$

and the typical experimental values given in the literature for 5CB (pentylcyanobiphenyl): $\gamma=1.5\times10^{-2}$ erg/cm^2, $\alpha=\beta\simeq0.1$ P, $\rho=1$ g/cm^3, $K=2.1\times10^{-7}$ dyn, $W_a=5\times10^{-4}$ erg/cm^2, and $S_{\mathrm{nem}}=0.35$ [13,20,21].

Three regions must be clearly distinguished.

In the short wavelength limit (region III in Fig. 1), the interface is diffuse as the relaxation of the order parameter in the inner region is the dominant process. The dispersion relation is then given by Eq. (56) (dotted curve in Fig. 1).

In the large wavelength limit, the interface is sharp and can be considered as a surface of discontinuity. The viscous damping processes in the outer region then dominate and the corresponding dispersion relation is given by Eq. (44) (dashed curve in Fig. 1). The transition between these two regimes takes place when $\mathrm{Re}(\Omega_{\eta\alpha})=\mathrm{Re}(\Omega_S)$, which gives the critical wave number $k_c\simeq5\times10^4$ cm^{-1} and the corresponding critical wavelength $\lambda_c\simeq1.2$ μm. It also appears immediately that the curve in Fig. 1 has a slope discontinuity marked by a small peak for a particular value of the wave number $k_*\simeq0.8$ cm^{-1}. So, two regions must be further distinguished in the hydrodynamic limit. The region I corresponds to $k<k_*$ where the nematic behaves as an isotropic liquid of viscosity $\eta=(\alpha+2\beta)/2$. This viscosity correspond to the second viscosity of Miesowicz (η_b according to standard notation [13]), i.e., to the viscosity of the nematic phase when it is sheared parallel to the director. Finally, the intermediate region II corresponds to $k_*<k<k_c$. In this range of wave vectors, the slope of the curve is smaller than in region I, which indicates a decrease of the dissipation. In this regime, curvature elasticity and backflow effects play an important role and cannot be ruled out.

To sum up, three distinct regions appear in Fig. 1: two regions in the hydrodynamic regime where the nematic behaves as an isotropic liquid of effective viscosity η when $k<k_*$ (region I), whereas for $k_*<k<k_c$ (region II), nematic effects become important. Finally, at large wave numbers $k>k_c$ (region III) the relaxation of the order parameter governs the physics. In order to better characterize these three regions we compare in the following section the results obtained in the general case with those obtained in the simplified model assuming $W_a=0$ and $\alpha=0$.

V. COMPARISON WITH THE CASE $W_a=0$ AND $\alpha=0$

It is interesting to compare these results with those obtained in Ref. [1] where it was assumed that the orientation of the director is fixed. As we have already mentioned, this assumption is correct if the surface tension is isotropic ($W_a=0$) and the coupling between the director and the flow is negligible (in our notation, this happens if $\alpha\ll\beta$ or $\alpha=0$).

In order that this comparison makes sense, we performed again the calculation of the dispersion relation by taking the same surface tension, which imposes to take the same value for L. This way, we have obtained $L_1=3.69\times10^{-7}$ dyn, $L_2=0$, $K_4=-K/2=-1.02\times10^{-7}$ dyn, $K_{eff}=0$, $b=2.03\times10^{-5}$ cm, and $\Omega_S=6.77\times10^{-7}k^2$.

In the following, we call Ω' the relaxation rate at $W_a=0$ and $\alpha=0$ (as calculated in Ref. [1]),

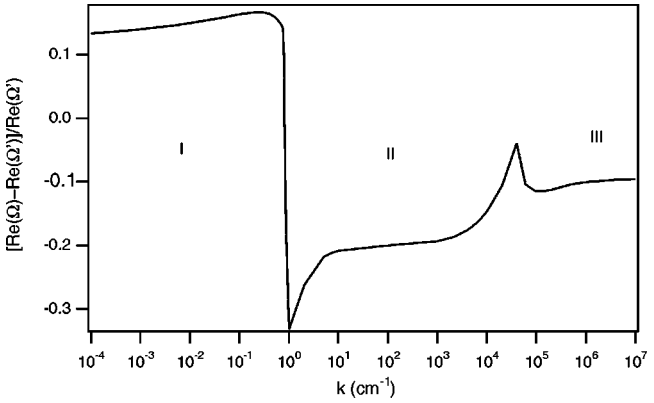

FIG. 2. The relative variation of the relaxation rate. The meaning of the three regions is the same as in Fig. 1.

$$\Omega'^2 - \Omega'_S \Omega' = \Omega_\beta^2, \tag{59}$$

where

$$\Omega'_S = \frac{2L_1}{3\mu_1} k^2 = 6.77 \times 10^{-7} k^2, \tag{60}$$

and Ω_β is given by Eq. (45).

In Fig. 2 we have plotted the relative variation of the relaxation rate $[\mathrm{Re}(\Omega) - \mathrm{Re}(\Omega')]/\mathrm{Re}(\Omega')$ as a function of k. Again the three regions discussed in the preceding section are clearly visible. In addition, we note that the relaxation rate is enhanced (with respect to the simplified case $\alpha = W_a = 0$) in region I, whereas it is lowered in regions II and III.

In Fig. 3 we have plotted $\mathrm{Im}(\Omega)$ and the corresponding phase velocity $v_p = \mathrm{Im}(\Omega)/k$ as a function of k in the two cases. In the two graphs, the general solution obtained from Eq. (57) is represented by the solid curves, while the dotted ones represent the solution obtained in the simplified case corresponding to Eq. (59). Again the three regions are clearly distinguishable. In region I, the phase velocities (or the imaginary parts of Ω) are almost identical, the difference coming from the difference of viscosity of the nematic phase in the two cases [equal to $(2\beta + \alpha)/2$ in the general case and to the smaller value β in the simplified case, which explains the difference]. On the other hand, there is a big qualitative difference in region II since $\mathrm{Im}(\Omega)$ (and then the phase velocity) are different from 0 in the general case, whereas they vanish in the simplified case. Note that $\mathrm{Im}(\Omega)$ and the phase velocity are zero in both cases in region III.

Finally, we have studied the effect of the surface tension anisotropy in the general case. For doing this, we have plotted in Fig. 4 the relative variation of the relaxation rate $[\mathrm{Re}(\Omega)(W_a \neq 0) - \mathrm{Re}(\Omega)(W_a = 0)]/\mathrm{Re}(\Omega)(W_a = 0)$. We note that the influence of W_a is null in the region I and becomes visible (although very small) in regions II (where it remains less than 4%) and III (where it goes up to 10%). In addition, we have plotted the phase velocities in both cases in Fig. 5. Because there is only a difference between the two cases in region II, we have restricted our graph to this region. Again the effect of the anisotropy is quite small, and is only visible close to the maximum of the curve which is slightly

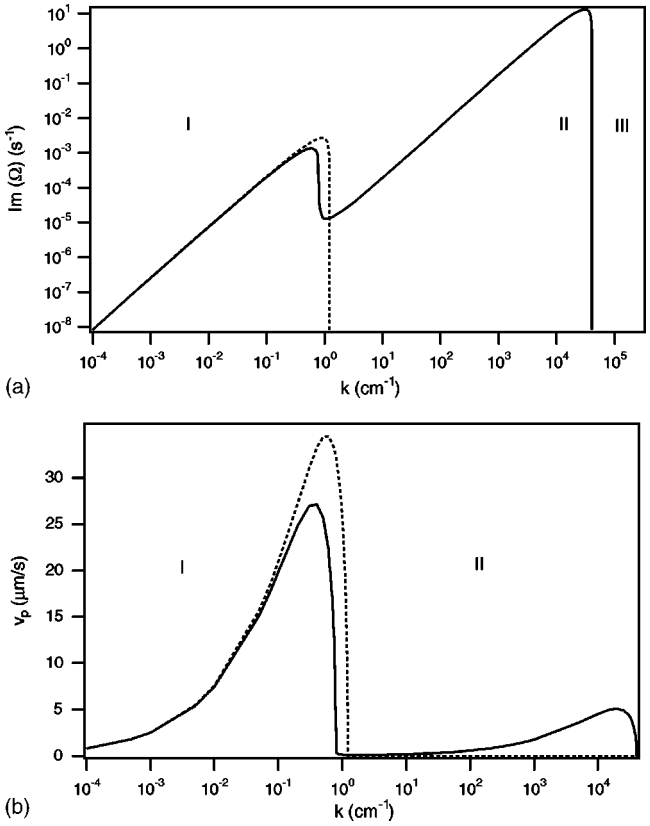

FIG. 3. $\mathrm{Im}(\Omega)$ (a) and corresponding phase velocities $v_p = \mathrm{Im}(\Omega)/k$ (b) calculated from Eqs. (57) (continuous curves) and (59) (dotted curves).

shifted towards the large values of k when $W_a \to 0$. These two figures show that the effect of the anisotropy is very small in comparison with the effect of the rotational viscosity α.

In the following section we discuss these results and give some analytical expressions which allow us to predict a few limiting cases showed in the previous graphs.

VI. DISCUSSION

We first discuss the region I (the limit $k \to 0$). In this limit, the nematic behaves almost as an ideal fluid, which means

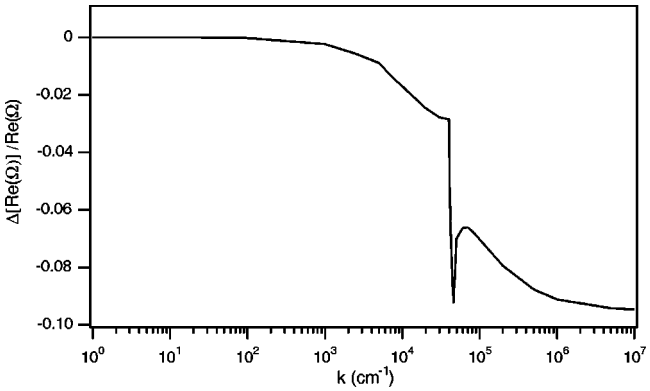

FIG. 4. The relative variation of the relaxation rate $[\mathrm{Re}(\Omega)(W_a \neq 0) - \mathrm{Re}(\Omega)(W_a = 0)]/\mathrm{Re}(\Omega)(W_a = 0)$.

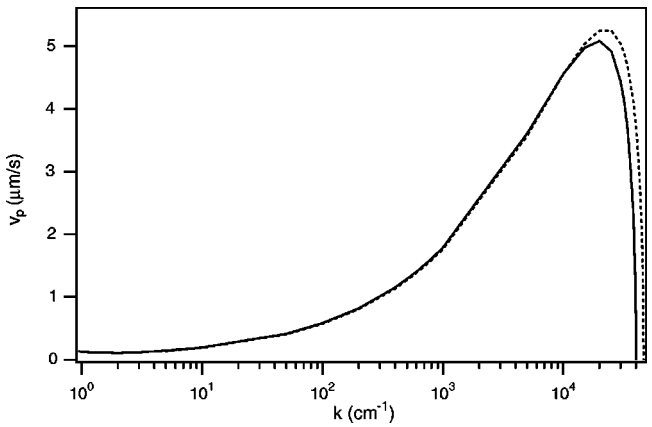

FIG. 5. The phase velocities. For $W_a = 5\times10^{-4}$ erg/cm^2 (experimental value), continuous curve and for $W_a = 0$, dotted curve.

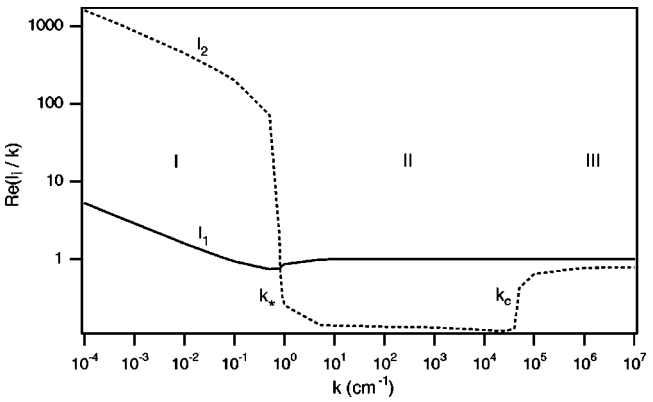

FIG. 6. Spatial attenuation lengths of the waves in the nematic phase as a function of the wave number.

that curl $\mathbf{n}=\mathbf{0}$. As a consequence the second term on the rhs of Eq. (28) vanishes which gives from the same equation $\alpha\phi\Omega \sim Kk^2\phi$. We conclude that the α terms on the rhs of Eqs. (26) and (27) (of the order of $\alpha k\Omega\phi \sim Kk^3\phi$) are completely negligible with respect to the usual viscous terms in η in the same equations (of the order of $\eta k^2 v$). So, the dissipation due to the rotational motion of the director is negligible and the nematic behaves as an isotropic fluid. In this case the dispersion relation (44) reduces to that for two fluids with equal densities but different viscosities:

$$\Omega^2 = \left[1 + \frac{k(l^2+l_1^2)-2k^3}{(l+l_1)(k^2-ll_1)}\right]\Omega_0^2, \tag{61}$$

where $l_1 = k(1-\rho\Omega/\eta k^2)^{1/2}$, $l = k(1-\rho\Omega/\beta k^2)^{1/2}$, and $\Omega_0^2 = -\gamma k^3/2\rho$. These formulas allow us to predict the asymptotic value of $[\mathrm{Re}(\Omega)-\mathrm{Re}(\Omega')]/\mathrm{Re}(\Omega')$ given in Fig. 2 as $k\to 0$. Indeed, in this limit of very small damping ($|\Omega_0| \gg \eta k^2/\rho$), Ω differs from Ω_0 only by a small quantity $\delta\Omega_\eta$ with a real part given by

$$\mathrm{Re}(\delta\Omega_\eta) = \frac{\gamma^{1/4}}{2^{7/4}\rho^{3/4}}\eta_{eff}^{1/2}k^{7/4}. \tag{62}$$

In this equation, the effective viscosity coefficient is defined to be

$$\eta_{eff}^{1/2} = \frac{\beta+\eta}{\beta^{1/2}+\eta^{1/2}}, \tag{63}$$

with $\eta = (2\beta+\alpha)/2$ in the general case and $\eta=\beta$ in the simplified case. From Eq. (63), we calculate, in the limit $k\to 0$,

$$\frac{\mathrm{Re}(\Omega)-\mathrm{Re}(\Omega')}{\mathrm{Re}(\Omega')} = \frac{\eta_{eff}^{1/2}-\beta^{1/2}}{\beta^{1/2}} = 0.124. \tag{64}$$

This value is in very good agreement with that found numerically in Fig. 2. Note that $\mathrm{Re}(\Omega) > \mathrm{Re}(\Omega')$ because the viscosity η of the nematic phase is greater in the general case ($\alpha \neq 0$) than in the simplified one ($\alpha = 0$). Another consequence of this difference of viscosities is that, in region I, $\mathrm{Im}(\Omega)$ and the corresponding phase velocity are larger the smaller the viscosity is. This explains the shift between the two curves in the region I of Fig. 3.

We now discuss the crossover between regions I and II in the general case, when $\alpha \neq 0$. Assuming $\alpha=\beta$ (as in our numerical calculations), the solutions of the characteristic equation (30) are given by

$$q = k \quad q = l_1 = k\left(1-\frac{\rho}{\eta k^2}\Omega\right)^{1/2},$$

$$q = l_2 = k\left(1-\frac{2\alpha\beta}{K\eta k^2}\Omega\right)^{1/2}. \tag{65}$$

These formulas show that l_1 is associated with the usual shear flow and is characterized by the relaxation time of vorticity $\tau_\eta = \rho/\eta k^2 \simeq 6.67/k^2$ (in cgs units). In contrast, l_2 is associated with the rotational motion of the director and is associated with the characteristic relaxation time of the fluctuations of the director orientation $\tau_\alpha = 2\alpha\beta/K\eta k^2 \simeq 6.35\times10^5/k^2$). In Fig. 6 we have plotted $\mathrm{Re}(l_1/k)$ and $\mathrm{Re}(l_2/k)$ as a function of k. The three regions are again clearly visible. In particular, this graph shows that the passage from the region I to the region II takes place at $k=k_*=0.812$ cm^{-1}, precisely when $\mathrm{Re}(l_2)=\mathrm{Re}(l_1)$. We emphasize that the two propagating modes observed in regions I and II are very well decoupled (see, in particular, in Fig. 3) because $\tau_\eta \ll \tau_\alpha$.

Finally, let us discuss the region III which is dominated by the dynamics of the order parameter. In that case, surface undulations are strongly damped and do not propagate. The dispersion relation is given by Eq. (56) which allows us to calculate the large wave numbers limit ($k\to\infty$) in the graph of Fig. 2:

$$\frac{\mathrm{Re}(\Omega_S)-\mathrm{Re}(\Omega_S')}{\mathrm{Re}(\Omega_S')} = -0.095. \tag{66}$$

Note that this limit is the same in the graph of Fig. 4.

VII. ABOUT EXPERIMENTS AND THE WAY TO MEASURE THE DISPERSION RELATION

In this section, we briefly review the experiments already performed on the nematic-isotropic interface and we recall a few general methods to measure the dispersion relation of capillary waves.

First of all, the surface tension of the nematic-isotropic interface has been measured [23]. One method consisted of analyzing the shape of a macroscopic (size in centimeter) nematic drop placed on a Teflon plate, itself situated in a transparent recipient filled with the isotropic liquid. Due to the gravity and the small density difference between the two phases, the drop slightly departs from its perfect spherical shape (the so-called ''sessile drop'' method [24]), allowing the determination of the surface tension (for the preferred orientation of the director at the interface). Unfortunately, this static experiment gives no information about capillary waves. On the other hand, it could be interesting to look at the mechanically excited deformation modes of a large drop in this type of system to explore the dispersion relation in regime I and obtain an estimate of the wave vector at which ''ordinary'' capillary waves are overdamped and stop propagating.

Another method to probe regime I would be to prepare a flat nematic-isotropic interface in a large recipient (many centimeters in size). The experimental procedure would then consist of mechanically (or electrically) exciting ''plane'' surface waves at a fixed frequency $f=2\pi/\omega$. In this case, the wave vector of the waves is complex $[q=\mathrm{Re}(q)+i\mathrm{Im}(q)]$. Each component of q can then be measured by observing the deflection of a laser beam with a position sensitive photodiode as a function of the distance to the excitation point. These two components are then compared to the solution (in q at fixed $\Omega=\omega$) of the dispersion relation. Note that this method has already been used for studying capillary waves at the nematic-air interface in regime I [25].

Another set of experiments on the nematic-isotropic interface has been performed by Faetti and Palleschi [21]. In that case, the reflectivity of the interface has been measured. This method allows a precise determination of the ''optical'' width of the interface. This quantity depends both on the ''static'' width of the interface [given by the Landau–Ginzburg–de Gennes theory and equal to $\sqrt{2}l_S$ according to Eq. (50)] and on its ''thermal'' width (in general much larger) [26]. The latter is due to thermal fluctuations which excite capillary waves at the interface. Thus, this method gives average information on the interface fluctuations. Note that, in this experiment, wave vectors which contribute to the reflectivity range from $1/\sqrt{2}l_S \sim 7\times10^5$ cm^{-1} down to $\alpha n/\lambda \sim 300$ cm^{-1}, where λ is the wavelength of the light in vacuum, n the sum of the refractive indices of the isotropic and of the nematic phases, and α some angle (of the order of $5\sim7\times10^{-3}$) fixed by the experimental setup. So, this experiment brings into play capillary waves of regimes II and III defined previously. On the other hand, it again gives no information about their dynamics.

To obtain direct information about dynamics of capillary waves, quasielastic laser light scattering can be used. This classical technique has been successfully performed for probing waves at liquid interfaces such as the water- *n* dodecane interface [27] or the liquid-vapor interface of the carbon dioxide very close to the critical point [28]. The latter example resembles the present case in both, the small density difference between the two phases and the very low surface tension. The nematic-air interface has also been investigated experimentally by light scattering [29,30] but this case is paradoxically closer to that of usual liquid-air interfaces than to ours. Briefly, the technique consists of measuring the power spectrum $P(k,\omega)$ of the scattered light at different wave vector k by using an heterodyne detection (for more details see Refs. [31,32]). To a first approximation, the spectrum is Lorentzian of half width $\mathrm{Re}[\Omega(k)]$ and it is shifted by $\mathrm{Im}[\Omega(k)]$ (Doppler effect due to the wave propagation). Wave vectors accessible experimentally range between 100 cm^{-1} and 10^4 cm^{-1}, which turn out to be in the regime II of the present study. Nevertheless, it must be noted that in this range of wave vector, $\mathrm{Im}(\Omega)$ is typically ten times smaller than $\mathrm{Re}(\Omega)$ (Fig. 7). For this reason, $\mathrm{Im}(\Omega)$ will be difficult to measure. One way to improve the situation consists of decreasing the viscosity in order to increase the phase velocity of the waves while decreasing their damping. From this point of view, 5CB is certainly not the best candidate for this experiment, as its nematic-to-isotropic transition temperature is pretty low. Let us now return to the nematic-air interface. In this case, the surface tension is typically three orders of magnitude larger than at the nematic-isotropic interface. Consequently, regime I at the nematic-air interface (the only one calculated by Langevin and Bouchiat [29,30]) extends up to values of k of the order of 10^3 cm^{-1}. That means that the nematic-air interface must roughly behave in light scattering as an ordinary liquid-air interface. The main difference with respect to an ordinary liquid is that the damping rate of the capillary waves depends on the orientation of the director with respect to the wave vector, as the viscosity depends on the orientation of the director with respect to the velocity and the velocity gradient. This obviously applies if the anchoring is not homeotropic (contrary to what we have assumed to simplify the calculations). It was indeed the case in the experiment of Langevin [30], who was able to extract from her measurements the surface tension and three distinct

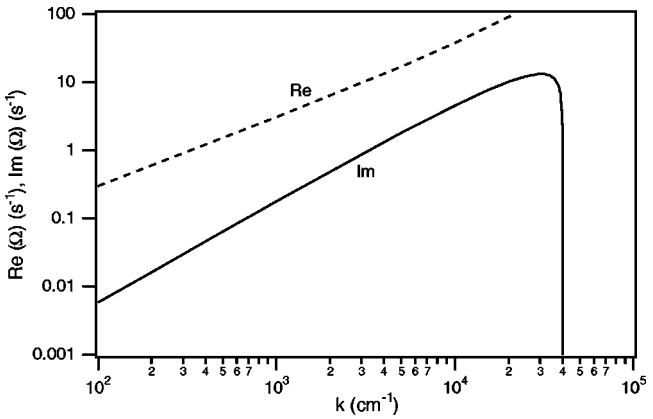

FIG. 7. $\mathrm{Re}(\Omega)$ and $\mathrm{Im}(\Omega)$ as a function of k in the range of wave vectors accessible by light scattering.

viscosities of the nematic phase. On the other hand, regime II, where curvature elasticity and backflow effects are important, is out of reach by light scattering at the nematic-air interface.

As for the region of transition between regimes II and III, which is predicted to appear at a wave vector of the order of 5×10^4 cm^{-1}, it should be accessible by diffuse scattering of x rays at grazing incidence. In particular, a photon correlation spectroscopy experiment should give valuable information in this region where dynamics of the order parameter become dominant.

Finally, we suggest that the Faraday instability could also be used to study capillary waves at the nematic-isotropic interface. We recall that this method consists of exciting parametrically capillary waves by vibrating a recipient containing the liquid crystal in the direction perpendicular to the interface. Because this experiment has already been performed at the liquid-vapor interface of the carbon dioxide close to the critical point [33], we believe it should be feasible in nematics and provide information about capillary waves in regimes I and II. In particular, we predict that the instability should disappear at the passage between regimes I and II.

VIII. CONCLUSIONS

In this paper (which can be regarded as a generalization of Ref. [1]) we have examined surface modes at the nematic-isotropic interface using the Qian and Sheng [9] generalized dynamical Landau–de Gennes theory. We have assumed an isothermal system characterized by a tensorial order parameter, both phases having the same density. Considering the surface tension anisotropy (the L_2 term in the elastic free energy density), we have also taken into account the coupling between interface oscillations, the director field, and velocity (by including backflow effects). We have considered the equilibrium planar nematic-isotropic interface as the base state of the system. The front was then perturbed with a small-amplitude monochromatic plane wave and the linear stability of the front was examined to obtain the generalized dispersion relation, Eq. (57). Three distinct regions can be distinguished (see Fig. 1): (i) at very low values of k ($k<k_*\approx1$ cm^{-1}) the dissipation due to shear flow dominates and the nematic behaves as a viscous isotropic fluid (region I), (ii) at intermediate values of k ($k_*<k<k_c\approx5\times10^4$ cm^{-1}) curvature elasticity and backflow effects become important (region II), and finally (iii) at large values of k ($k>k_c$) the relaxation of the order parameter governs the physics (region III).

We compared these results with those obtained in Ref. [1] where it was assumed that the orientation of the director is fixed. The influence of the anisotropy of the surface tension and of the hydrodynamic coupling between the flow and the director has a fairly small effect ($\simeq-20\%$) on the relaxation rate; in contrast, this influence on the phase velocity is very important in region II in which a new propagating mode is observed (see Figs. 2 and 3.) We have also compared the effect of anchoring energy to that of rotational viscosity on these two quantities (see Figs. 4 and 5) finding that the effect of the rotational viscosity and associated backflow effect is much more important than that of the anchoring energy.

Finally, we have proposed experiments to examine and study these three regimes. Of course, our calculations are simplified as we do not use the complete set of Leslie viscosities and we assume isotropic curvature elasticity. Nevertheless, we think that the physics is preserved in the general case, in which only a numerical calculation can give the full dispersion relation. Another simplication concerns the anchoring at the interface. We have treated the homeotropic case, but we know from experiments (see, for instance, Ref. [21]) that the molecules are often tilted with respect to the normal to the interface. This type of anchoring cannot be explained in the framework of the present theory, which consequently must be completed by adding some new ingredients such as ordoelectricity [34]. This complication, again, should not change the nature of the problem, but could lead to new phenomena as it breaks the rotational invariance about the axis perpendicular to the normal to the interface. Indeed, assume that the molecules form an angle Φ different from 0 and $\pi/2$ with the z axis and are inclined in the direction $x>0$. In this case, waves propagating along the x axis should have different phase velocities in the regime II according to whether they propagate in one direction or in the opposite one. As a consequence, the power spectrum observed in light scattering should not be symmetric in k and $-k$. Another complication that can arise concerns the formation of an interface instability in oblique anchoring. This instability can lead to an array of umbilics or to the formation of a hill-and-valley structure when a magnetic field (which, in principle, could be included in the calculation of the dispersion relation) is imposed to obtain a homogeneous orientation of the sample. Nevertheless, we emphasize that these instabilities can be avoided easily provided that the nematic layer thickness be larger than some critical thickness, which depends on the temperature gradient applied perpendicularly to the interface (for an estimate, see Ref. [13]).

ACKNOWLEDGMENTS

V.P.-N. acknowledges support from Rhône-Alpes and CNRS grants and thanks the Ecole Normale Supérieure de Lyon for scientific hospitality. We thank V. Bergeron for fruitful discussions.

[1] V. Popa-Nita and T.J. Sluckin, Phys. Rev. E **66**, 041703 (2002).
[2] For a review of phase-field models, see, e.g., A.A. Wheeler, J. Stat. Phys. **95**, 1245 (1999).
[3] V. Popa-Nita and T.J. Sluckin, J. Phys. II **6**, 873 (1996); V. Popa-Nita, T.J. Sluckin, and A.A. Wheeler, *ibid.* **7**, 1225 (1997).
[4] P. Ziherl, A. Šarlah, and S. Žumer, Phys. Rev. E **58**, 602 (1998); A. Šarlah and S. Žumer, *ibid.* **60**, 1821 (1999).

[5] P.G. de Gennes, Mol. Cryst. Liq. Cryst. **12**, 193 (1971).
[6] For a review of these models, see, e.g., T. J. Sluckin and A. Poniewierski, in *Fluid Interfacial Phenomena*, edited by C. A. Croxton (Wiley, New York, 1986), Chap. 5; B. Jérôme, Rep. Prog. Phys. **54**, 391 (1991).
[7] S. Hess, Z. Naturforsch. A **31**, 1507 (1976).
[8] P.D. Olmsted and P. Goldbart, Phys. Rev. A **41**, 4578 (1990); **46**, 4966 (1992).
[9] T. Qian and P. Sheng, Phys. Rev. E **58**, 7475 (1998).
[10] J.L. Ericksen, Arch. Ration. Mech. Anal. **4**, 231 (1960).
[11] F.M. Leslie, Q. J. Mech. Appl. Math. **19**, 357 (1966); Arch. Ration. Mech. Anal. **28**, 265 (1968).
[12] P. G. de Gennes and J. Prost, *The Physics of Liquid Crystals*, 2nd ed. (Oxford University Press, Oxford, 1993).
[13] P. Oswald and P. Pieranski, *Les Cristaux Liquides: Concepts et Propriétés Physiques Illustrés Par Des Expériences* (Gordon and Breach, Paris, 2000), Vol. 1.
[14] E.F. Carr, Mol. Cryst. Liq. Cryst. **34**, 159 (1977).
[15] E. Guyon, R. Meyer, and J. Salan, Mol. Cryst. Liq. Cryst. **54**, 261 (1979).
[16] L. D. Landau and E. M. Lifshitz, *Fluid Mechanics* (Pergamon Press, Oxford, 1959).
[17] V. G. Levich, *Physicochemical Hydrodynamics* (Prentice-Hall, Englewood Cliffs, NJ, 1962).
[18] U.-Ser Jeng, L. Esibov, L. Crow, and A. Steyerl, J. Phys.: Condens. Matter **10**, 4955 (1998).
[19] J. Jäckle, J. Phys.: Condens. Matter **10**, 7121 (1998).
[20] N.V. Madhusudana and R. Pratibha, Mol. Cryst. Liq. Cryst. **89**, 249 (1982).
[21] S. Faetti and V. Palleschi, J. Chem. Phys. **81**, 6254 (1984); Phys. Rev. A **30**, 3241 (1984); J. Phys. (France) Lett. **45**, L313 (1984).
[22] J.S. Langer, Ann. Phys. **41**, 108 (1967); J. Zittartz, Phys. Rev. **154**, 529 (1967); A.J. Bray, Phys. Rev. E **58**, 1508 (1998); W. van Saarloos, Phys. Rep. **301**, 9 (1998).
[23] R. Williams, Mol. Cryst. Liq. Cryst. **35**, 349 (1976).
[24] A. W. Adamson, *Physical Chemistry of Surfaces* (Wiley Interscience, New York, 1990).
[25] C.H. Sohl, K. Miyano, J.B. Ketterson and G. Wong, Phys. Rev. A **22**, 1256 (1980).
[26] J. Meunier and D. Langevin, J. Phys. (France) Lett. **43**, L185 (1982).
[27] S. Hard and R.D. Neuman, J. Colloid Interface Sci. **115**, 73 (1987).
[28] M.A. Bouchiat and J. Meunier, Phys. Rev. Lett. **23**, 752 (1969); J. Phys. (France) **32**, C5a-181 (1971).
[29] D. Langevin and M.A. Bouchiat, J. Phys. (France) **33**, 101 (1972).
[30] D. Langevin, J. Phys. (France) **37**, 901 (1976).
[31] For a review about experimental studies of liquid at interfaces, see J. Meunier, in *Liquids at Interfaces*, Proceeding of the Les Houches Summer School, Session XLVIII, edited by J. Charvolin, J.-F. Joanny, and J. Zinn-Justin (North-Holland, Amsterdam, 1988).
[32] For the description of a simple apparatus allowing the study of capillary waves at a liquid surface through the quasielastic scattering of light, see W.M. Klipstein, J.S. Radnich, and S.K. Lamoreaux, Am. J. Phys. **64**, 758 (1996).
[33] S. Fauve, K. Kumar, C. Laroche, D. Beysens, and Y. Garrabos, Phys. Rev. Lett. **68**, 3160 (1992).
[34] G. Barbero, I. Dozov, J.F. Palierne, and G. Durand, Phys. Rev. Lett. **56**, 2056 (1986).